The use of molecular beam epitaxy for the synthesis of high purity III–V nanowires

2008 J. Phys.: Condens. Matter 20 454225

(http://iopscience.iop.org/0953-8984/20/45/454225)

J. Phys.: Condens. Matter **20** (2008) 454225 (5pp) doi:10.1088/0953-8984/20/45/454225

The use of molecular beam epitaxy for the synthesis of high purity III–V nanowires

D Spirkoska[1], C Colombo[1], M Heiss[1], G Abstreiter and A Fontcuberta i Morral

Walter Schottky Institut, Technische Universität München, D-85748 Garching, Germany

Received 16 May 2008, in final form 11 October 2008
Published 23 October 2008
Online at stacks.iop.org/JPhysCM/20/454225

Abstract
The synthesis methods and properties of catalyst-free III–V nanowires with molecular beam epitaxy (MBE) are reviewed. The two main techniques are selective-area epitaxy (SAE) and gallium-assisted synthesis. The excellent structure and ultra-high purity characteristics of the grown nanowires are presented by Raman and photoluminescence spectroscopy.

(Some figures in this article are in colour only in the electronic version)

1. Introduction

Semiconductor nanowires constitute extremely promising building blocks for 21st century electronic and optoelectronic devices. One reason is that their size will enable further downscaling of electronics [1–4]. A second reason is that nanoscale objects exhibit new properties which, at the same time, can be exploited into new device concepts such as high mobility transistors, thermoelectric applications and/or solar cells [5–8]. As a consequence, fundamental and applied research on nanowires has increased dramatically in the last few years.

One issue of crucial importance has been the control of the crystalline quality and impurity concentrations, as well as the reproducibility of the structures. With regards to purity, one of the key issues has been to avoid the use of gold as a nucleation and growth seed of the nanowires. Gold is a fast-diffusing metal that significantly harms the properties of semiconductors [9]. To date, synthesis without gold has been achieved by the use of alternative metals such as aluminum and titanium, or by simply avoiding the use of a catalyst [10–13].

Traditionally, molecular beam epitaxy (MBE) has been one of the oldest techniques applied to the fabrication of high quality nanostructures. Combining the high purity of MBE with growth methods that avoid the use of gold will eventually lead to the synthesis of nanowires with superior structural quality, which is the subject of study of this paper. The main focus is given to two different techniques: selective-area epitaxy (SAE) and group III assisted growth.

The purpose of SAE is to restrict the incorporation of the adatoms into certain areas on a patterned substrate. Basically, the III–V substrate is masked with a patterned SiO_2 layer and growth conditions are appropriately chosen to restrict the epitaxial growth inside the apertures. This technique has been used in both metal–organic chemical vapor deposition (MOCVD) and MBE [18, 14–16]. In MOCVD the selectivity originates from a preferential decomposition of the metal–organic precursors on III–V surfaces with respect to the SiO_2. In the case of MBE, the selectivity originates from the lowering of the sticking coefficient of the species on the oxide, in comparison to the open III–V surfaces.

A fundamentally different method to obtain III–V nanowires is based on the vapor–liquid–solid method, in which a metal droplet is used to gather and precipitate the growth precursors. Typically, gold is a metal that works relatively well for any material. Instead, in principle it should be possible to use group III metal droplets to gather group V elements and precipitate III–V nanowires underneath. In the case of GaAs nanowires, this leads to what we call '*gallium-assisted growth*', but the method can be extended to other III–V combinations such as InAs, InGaAs and AlAs. It is intuitively clear that the growth conditions leading to this kind of growth have to be group III-rich. For simplicity, we will just discuss the case of GaAs and therefore call these conditions Ga-rich.

After introducing the growth methods the rest of the paper is structured as follows. First the experimental conditions leading to growth of nanostructures by SAE and Ga-assisted growth are given. The structural and optical characterizations will follow. Finally, the paper is concluded.

2. Experimental details

The samples were grown in a high purity Gen-II MBE system. In all cases, two-inch GaAs wafers sputtered with a 10–50 nm

[1] Equal contribution.

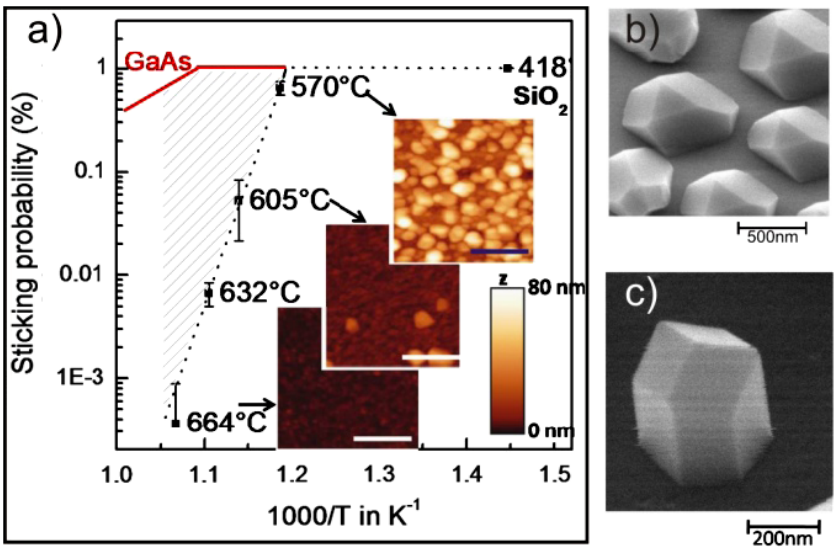

Figure 1. (a) Measured sticking probability of GaAs on SiO_2 a function of temperature. In the insets atomic force micrographs of the surfaces after deposition of 50 nm of GaAs are shown. The scale bar stands for 400 nm. (b) and (c) represent scanning electron micrographs of 200 nm GaAs grown on (111) A and (111) B GaAs substrates, respectively.

thick silicon dioxide film were used as substrates. In the case of selective-area epitaxy, the oxide was patterned with holes by combining lithography with reactive ion etching [17]. In the case of gallium-assisted growth of nanowires, no patterning was realized on the surface.

In order to ensure a contamination-free surface, prior to the introduction into the MBE chamber the substrates were dipped for 2 s in a buffered HF aqueous solution (10% HF). In order to desorb any remnant adsorbed molecules of the surface, the wafers were heated to 650 °C for 30 min prior to growth.

2.1. Selective-area epitaxy

We present first a study on the selective desorption of the Ga adatoms on SiO_2 surfaces by measuring the temperature dependence of the sticking coefficient, s, of GaAs on SiO_2. s is a measure of the probability of an adatom to precipitate, forming a film instead of desorbing. It can be simply measured by comparing the nominal thickness with the actual thickness of material that has grown on the substrate. A nominal thickness of 50 nm GaAs was grown on SiO_2 at temperatures ranging between 418 and 664 °C. The GaAs growth rate, as calibrated on GaAs at 550 °C, was 0.4 Å s^{-1}. The morphology of the surface after deposition was analyzed by atomic force microscopy and scanning electron microscopy (AFM and SEM, respectively). In figure 1(a) the results on the sticking coefficient of GaAs on SiO_2 (s_{SiO_2}) as a function of temperature are presented and compared to the literature values for GaAs on GaAs (s_{GaAs}) [18]. The AFM of the surfaces after depositing nominally 50 nm of GaAs are also shown for illustration in the inset. For temperatures below 565 °C, s is close to 1 in both cases, meaning that 100% of the Ga adatoms precipitate on the oxide surface. For temperatures above 565 °C, s_{SiO_2} starts to decrease and stays well below the value on GaAs. This means that for these temperatures, the fraction $(1-s)$ of Ga adatoms desorb from the surface. Finally, at temperatures higher than 650 °C, s on SiO_2 is very close to zero, meaning that deposition of GaAs is not possible.

We have grown different thicknesses of GaAs on patterned substrates, at 650 °C. Different substrate orientation has been used in order to compare the morphology of the obtained structures. For deposited thicknesses below 100 nm, the growth in the openings occurs in a planar way and no significant difference is observed between the substrates. However, for higher nominal thicknesses the grown pillars develop clearly defined facets that are always defined in terms of the minimization of energy. According to our results and the existing literature, the facets with lowest formation energy are those of the family {110} and {111}, as well as sometimes {311}. In figures 1(b) and (c) scanning electron microscopy (SEM) of structures grown by SAE on (111)A and (111)B GaAs patterned substrates are shown. Clearly the geometry of the faceting is significantly different. Due to the perpendicularity between (111)B and $(1\bar{1}0)$ facets, only in the case of (111)B substrates is a vertical growth in the form of nanowires possible. In the other cases, the faceting leads into pyramidal or multi-polyhedral structures.

2.2. Ga-assisted growth

As was discussed in the introduction, in order to achieve growth of GaAs nanowires by the Ga-assisted growth method the growth must be done in Ga-rich conditions. In order to find the right conditions, it is necessary to look at the gallium and arsenic partial pressures of GaAs as a function of temperature. The schematic of this diagram is shown in figure 2(a) [19, 20].

For temperatures below 630 °C, the vapor pressures of Ga and As equilibrate the stoichiometry of GaAs to 50% of each element. At higher temperatures, this balance is not possible because the partial pressure of As is higher.

In practice, this leads to the selective evaporation of As, which in turns results in the formation of Ga droplets at the

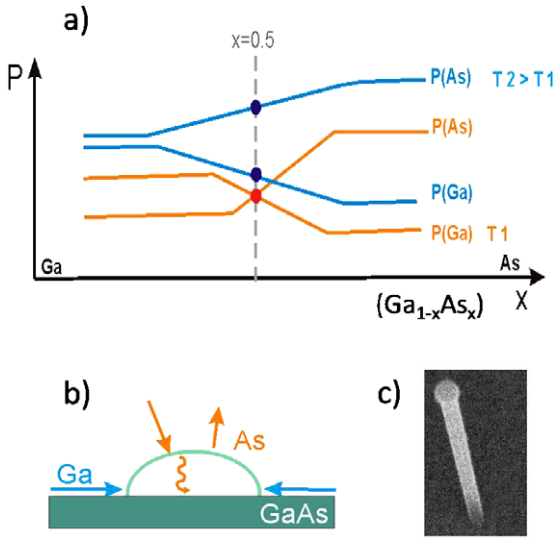

Figure 2. (a) Partial pressures of Ga and As at the GaAs surface as a function of temperature. For temperatures higher than 630 °C precipitates of Ga form at the GaAs surface. T_1 stands for temperatures lower than the congruent temperature while T_2 denotes higher temperatures than the congruent. (b) Schematic of Ga droplet in equilibrium with GaAs surface. (c) Scanning electron micrograph of single GaAs nanowire. The Ga droplet is clearly observable at the top of the nanowire.

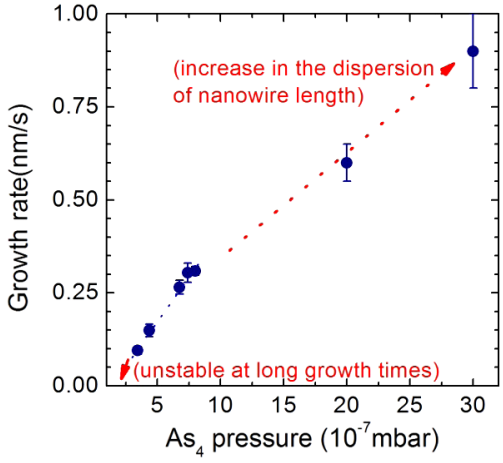

Figure 4. Dependence of the growth rate from the As beam pressure. The growth rate is unstable for pressures less than 3.5×10^{-7} mbar, while for pressures above 8×10^{-7} mbar the dispersion of the nanowires length is significantly increased. The dashed blue line is a result from a linear fit and the dashed red line is a guide to the eye.

surface. This transition temperature is commonly referred to as the congruent temperature [25]. The schematic of the equilibrium of the Ga droplet at the GaAs surface above the congruent temperature is presented in figure 2(b) while in figure 2(c) an SEM micrograph from a single nanowire with clearly observable droplet at the top is presented. In order to use these Ga droplets for the gathering of As and growth of GaAs nanowires, a further element has to be considered. Indeed, in order to avoid the spreading and increase of the Ga droplet, it is necessary to avoid the wetting of the metal on the surface. For this reason, direct growth on GaAs has to be avoided. Instead, we used GaAs substrates covered with a thin SiO_2 layer.

We have obtained GaAs nanowires by growing on SiO_2, under low arsenic beam fluxes, at 630 °C. We have observed that, when the oxide is thin enough (below 30 nm), the nanowires grow following the (111)B direction of the substrate [13]. This is shown in figure 3, where the scanning electron micrographs of nanowires grown on (001) and (111)B GaAs substrates are shown ((a) and (b), respectively). In one case, the wires grow, forming a 34° angle with the surface, while in the other case the wires grow perpendicularly.

In order to prove that the nanowire growth is governed by the arsenic, we investigated the effect of the arsenic beam flux on the growth rate of the GaAs nanowires. The results are shown in figure 4.

In agreement with our hypothesis, the growth rate is proportional to the arsenic beam flux in ranges from 3.5×10^{-7} to 3.5×10^{-6} mbar. For pressures below 3.5×10^{-7} mbar, the growth rate is very low and the growth is highly unstable. Between 3.5 and 8×10^{-7} mbar the dispersion in the nanowire growth rate is very small, while for higher beam pressures a large dispersion in the length exists. The reason for the increased size dispersion remains unclear, though one reason could be delayed incubation times among the nanowires. The growth rate of nanowires was also measured as a function of the Ga rate. In figure 5, the length of the nanowires as a function of time is plotted for different Ga rates, with an As beam pressure of 8×10^{-7} mbar.

It is clear that all points fall on the same line, indicating an identical growth rate for the Ga rates varying from 0.12 to

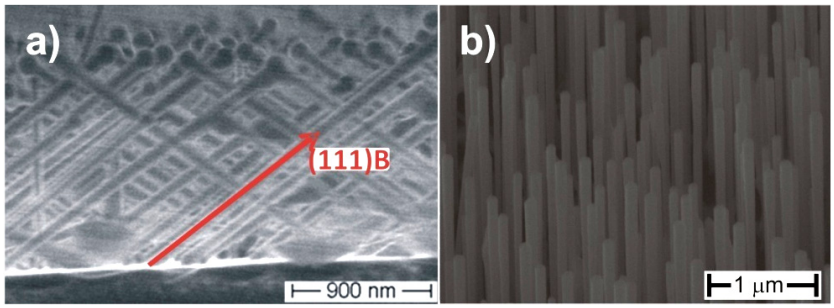

Figure 3. Scanning electron micrographs of GaAs nanowires grown on (a) (001) GaAs substrate and (b) (111)B GaAs substrate.

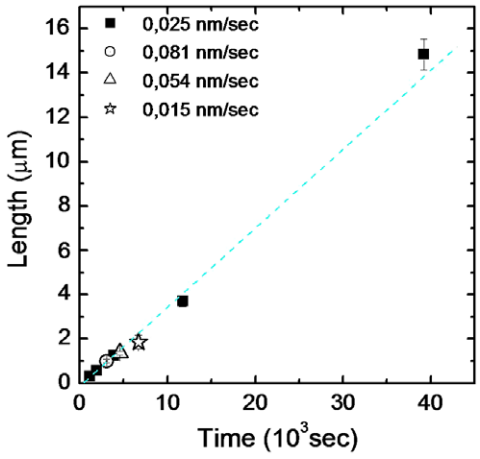

Figure 5. The length of the nanowires as a function of the growth time for different Ga arrival rates but constant value of the As beam pressure from 8×10^{-7} mbar. The points are experimental data while the dashed blue line is a result from a linear fit. Clearly the growth rate of the nanowires does not depend on the Ga arrival rate.

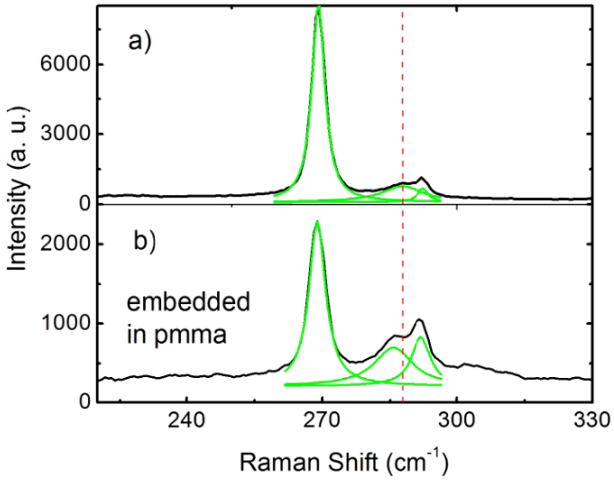

Figure 6. (a) Raman spectra from GaAs nanowires. The black line is the measured data while the lighter color lines are the result of a multiple Lorentzian fit. (b) Raman spectra from GaAs nanowires embedded in PMMA. A clear shift in the SO position is present. The red dashed line is a guide to the eye.

0.82 Å s^{-1}. This result indicates that under these conditions the growth of the nanowires is not limited by the amount of Ga adatoms arriving at the surface, as is usually the case in epitaxial growth of GaAs thin films [21].

3. Structural and optical properties

The structural properties of the GaAs nanowires were investigated by Raman spectroscopy. Prior to the measurements, bundles of nanowires were dispersed on a silicon substrate. The Raman experiments were performed at room temperature by using the 488 nm line from an Ar^+laser, focused with a 50× microscope objective. The measurements were realized with low excitation power (0.5 mW), in order to avoid heating the sample. As shown by the Stokes/antiStokes ratio measurements, the temperature of the nanowires remained below 120 °C.

A typical Raman spectrum of the nanowires is presented in figure 6(a). The solid black line is the recorded data while the green lines are the result from a multiple Lorentzian fit. The peak positioned at 268.7 cm^{-1} can be attributed to scattering from transverse optical phonons (TO) and the peak positioned at 292.2 cm^{-1} is due to scattering from longitudinal optical phonons (LO). The TO and LO peaks are symmetric and have very small FWHM (around 4 cm^{-1}). The peak position corresponds exactly with the position of the TO and LO peaks measured on bulk (111) GaAs. The measured values for the peak positions and FWHM are a good indication that the synthesized wires have excellent structural quality, free of defects and stress, which further corroborates the advantage of using MBE.

A third peak positioned at the low frequency side from the LO phonon is also clearly observed. As previous studies have shown, this peak can be attributed to scattering from surface optical phonons (SO) [22]. The surface-related nature of this mode can be proved by a simple experiment. Namely, as predicted by the theory the position of the SO phonon depends on the dielectric constant of the surrounding environment [22, 23]. For that reason the nanowires were embedded in a PMMA (polymethylmethacrylate) matrix which has a dielectric constant of 2.8. Indeed, as can be seen from figure 6(b) the change in the environmental dielectric constant leads to a shift of the SO position of 1.8 cm^{-1}. As an additional confirmation about the nature of this mode Raman measurements on nanowires with different average diameters were performed. It was observed that this mode downshifts with the decrease in diameter of the nanowires [24].

In order to further assess the quality of the nanowires, photoluminescence spectroscopy (PL) on single nanowires was realized at 4.2 K by means of a confocal microscope. The PL was excited using the 632.8 nm line of an He–Ne laser and detected by the combination of a grating spectrometer and a silicon charge-coupled device (CCD). For the measurements, the wires were dispersed on a silicon substrate. Single wires were localized by scanning reflectivity measurements on a 30×30 μm^2 area of the sample. An example is shown in figure 7(b), where the nanowire can be clearly identified in the middle of the scan. The PL emission of a single GaAs nanowire is shown in figure 7(a). The PL spectrum is characterized by a peak centered at 1.51 eV with a full width at half-maximum of 6 meV, which corresponds well to the free exciton of undoped bulk GaAs. It should be stressed that these data are exceptional among the nanowires and further corroborate the high crystalline quality and purity of the nanowires. Furthermore a spatially resolved PL (figure 7(c)) clearly shows that the wire emits along its entire length. Here it is also important to note that the wires were not passivated, meaning that there might be very few surface states (which may be related to the fact that the (110) GaAs surface has no bandgap states on the clean surface [25]). Subsequent passivation of the facets of the wires by layers of AlGaAs and GaAs resulted in an increase of the photoluminescence signal by 100 times.

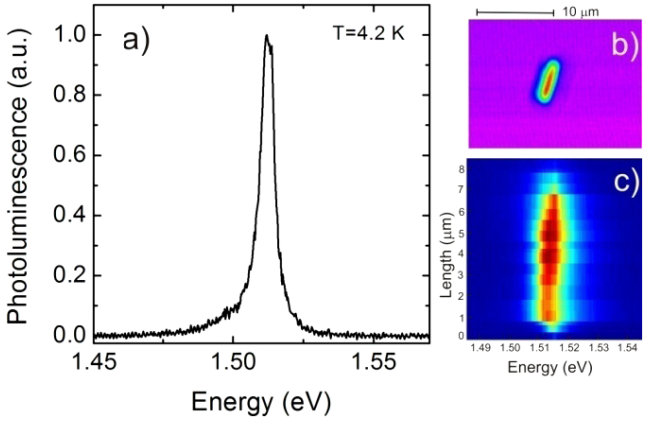

Figure 7. (a) PL spectra from single GaAs nanowires. The emission from the nanowires corresponds very well with emission from bulk GaAs. (b) Scanning reflectivity measurement on a small area of the sample. The single nanowire is clearly visible. (c) Spatially resolved PL. The wire emits along the entire length.

4. Conclusions

We have presented two methods for growth of GaAs nanowires by MBE. The influence of substrate orientation, beam pressure and the arrival rate of Ga atoms on the growth of nanowires was presented. We have shown that the Ga-assisted synthesis leads to synthesis of nanowires with ultra-high purity and excellent structural quality, as proved by Raman and PL spectroscopy.

Acknowledgments

The authors kindly thank D Grundler, R Gross, M Stutzmann, J R Morante and B Laumer for experimental support and discussions as well as M Bichler for helpful discussions on MBE. The financial support from the Marie Curie Excellence Grant SENFED, Nanosystems Initiative Munich (NIM) and SFB 631 is greatly acknowledged.

References

[1] Bjork T M, Hayden O, Schmid H, Riel H and Riess W 2007 *Appl. Phys. Lett.* **90** 142110
[2] Schmidt V, Riel H, Senz S, Karg S, Riess W and Goesele U 2006 *Small* **1** 85–8
[3] Chau R, Datta S, Doczy M, Doyle B, Jin J, Kavalieros J, Majumdar A, Metz M and Radosavljevic M 2005 *IEEE Trans. Nanotechnol.* **4** 153–8
[4] Knoch J, Riess W and Appenzeller J 2008 *IEEE Electron Device Lett.* **29** 372–4
[5] Lu W, Xiang J, Timko P B, Wu Y and Lieber M C 2005 *Proc. Natl Acad. Sci.* **19** 10046–51
[6] Guichard R A, Barsic N D, Sharma S, Kamins I T and Brongersma L M 2006 *Nano Lett.* **6** 2140–4
[7] Shi L, Li D, Yu C, Jang W, Kim D, Yao Z, Kim P and Majumdar A 2003 *J. Heat Transf.* **125** 881–8
[8] Maiolo R J, Kayes M B, Filler A M, Putnam C M, Kelzenberg D M, Atwater A H and Lewis S N 2007 *J. Am. Chem. Soc.* **129** 12346–7
[9] Brotherson D S and Lowther E J 1980 *Phys. Rev. Lett.* **44** 606
[10] Wang W Y, Schmidt V, Senz S and Gosele U 2006 *Nat. Nanotechnol.* **1** 186–9
[11] Kamins I T, Williams S, Basile P D, Hesjedal T and Harris S J 2001 *J. Appl. Phys.* **89** 1008–16
[12] Mandl B, Stangl J, Mårtensson T, Mikkelsen A, Eriksson J, Karlsson S L, Bauer G, Samuelson L and Seifert W 2006 *Nano Lett.* **6** 1817–21
[13] Morral A F I, Colombo C, Arbiol J, Morante R J and Abstreiter G 2008 *Appl. Phys. Lett.* **92** 063112
[14] Hong M J, Wang S, Sands T, Washburn J, Flood D J, Merz L J and Low T 1986 *Appl. Phys. Lett.* **48** 142–4
[15] Mohan P, Motohisa J and Fukui T 2005 *Nanotechnology* **16** 2903–7
[16] Mandl B, Stangl J, Martensson T, Mikkelsen A, Eriksson J, Karlsson S L, Bauer G, Samuelson L and Seifert W 2006 *Nano Lett.* **6** 1817–21
[17] Heiß M, Riedlberger E, Spirkoska D, Bichler M, Abstreiter G and Fontcuberta i Morral A 2008 *J. Cryst. Growth* **310** 1049–56
[18] Fisher R, Klem J, Drummond J T, Thorne E R, Kopp W, Morkoc H and Cho Y A 1983 *J. Appl. Phys.* 54 2058–510
[19] Chatillon C and Chatain D 1995 *J. Cryst. Growth* **151** 91–101
[20] Shen Y J and Chatillon C 1990 *J. Cryst. Growth* **106** 543–552
[21] Colombo C, Spirkoska D, Frimmer M, Abstreiter G and Morral A F I 2008 *Phys. Rev.* B **77** 155326
[22] Watt M, Sotomayor Torres M C, Arnot G E H and Beaumont P S 1990 *Semicond. Sci. Technol.* **5** 285
[23] Ruppin R and Englman R 1970 *Rep. Prog. Phys.* **33** 149–96
[24] Spirkoska D, Abstreiter G and Morral A F I 2008 *Nanotechnology* **19** 435704
[25] Van Laar J and Scheer J U 1967 *J. Surf. Sci.* **8** 342